Atmospheric temperature changes over the 20 th century at very high elevations in the European Alps from englacial temperatures

A. Gilbert, C. Vincent

Atmospheric temperature changes over the 20th century at very high elevations in the European Alps from englacial temperatures

A. Gilbert[1] and C. Vincent[1]

Received 17 January 2013; revised 19 March 2013; accepted 20 March 2013; published 23 May 2013.

[1] Given the paucity of observations, a great deal of uncertainty remains concerning temperature changes at very high altitudes over the last century. Englacial temperature measurements performed in boreholes provide a very good indicator of atmospheric temperatures for very high elevations although they are not directly related to air temperatures. Temperature profiles from seven deep boreholes drilled at three different sites between 4240 and 4300 m above sea level in the Mont Blanc area (French Alps) have been analyzed using a heat flow model and a Bayesian inverse modeling approach. Atmospheric temperature changes over the last century were estimated by simultaneous inversion of these temperature profiles. A mean warming rate of 0.14°C/decade between 1900 and 2004 was found. This is similar to the observed regional low altitude trend in the northwestern Alps, suggesting that air temperature trends are not altitude dependent. **Citation:** Gilbert, A., and C. Vincent (2013), Atmospheric temperature changes over the 20th century at very high elevations in the European Alps from englacial temperatures, *Geophys. Res. Lett.*, *40*, 2102–2108, doi:10.1002/grl.50401.

1. Introduction

[2] The altitude dependency of temperature trends is a key issue for climate change studies [*Intergovernmental Panel on Climate Change*, 2007]. It has been suggested that high-altitude regions may be more sensitive to global-scale climate change than other land surfaces at the same latitudes [e.g., *Messerli and Ives*, 1997; *Beniston et al*., 1997]. In the Alps, several studies using climate models have shown an elevation-dependent climate response [e.g., *Giorgi et al*., 1997, *Im et al*., 2010]. In contrast, studies based on ground observations in the Alps do not show a clear elevation dependency [*Ceppi et al*., 2010; *Rangwala and Miller*, 2012; *Beniston and Rebetez*, 1996; *Jungo and Beniston*, 2001]. However, most long-term meteorological data come from altitudes that do not exceed 3000 m a.s.l. (above sea level). In addition, several studies [*Ceppi et al*., 2010; *Pepin and Lundquist*, 2008] mention that the altitude dependency of surface temperature trends obtained from observations is likely to be influenced by local effects such as snow-albedo feedback and is not representative of temperature trends at a more global scale. Given that there is no long-term temperature series in the Alps for altitudes greater than 3500 m a.s.l. for which this feedback can be neglected (because of snow persistence all year round), the trends obtained from temperature data are difficult to interpret. The temperature-dependency question remains unsolved and, in their review, *Rangwala and Miller* [2012] suggest that both observations and models are currently inadequate to provide a clear understanding of climate change in high elevation regions.

[3] An essential requirement is to increase climate monitoring at very high elevation sites. Mountain summits or isolated saddles located above the 0°C isotherm all year round are the best locations to quantify climate change at high elevations because they are less influenced by topography or urbanization, and the snow-albedo feedback does not change significantly at these altitudes [*Pepin and Lundquist*, 2008]. Englacial temperatures within cold glaciers provide an excellent tool to investigate climate change in these areas and can be used as a proxy for temperature change where meteorological data are almost inexistent [*Lüthi and Funk*, 2001; *Vincent et al*., 2007b; *Gilbert et al*., 2010]. In the Mont Blanc (France) and Monte Rosa area (Switzerland, 4500 m a.s.l), englacial temperature observations show that temperature profiles are far from a steady state and show a strong warming since 1980 [*Lüthi and Funk*, 2001; *Vincent et al*., 2007b; *Hoelzle et al*., 2011]. The near surface firn temperatures depend on complex mass and energy exchanges at the snow surface but are mainly driven by air temperature and meltwater refreezing. This is physically based on the fact that firn surface temperature variations are similar to air temperature variations and energy transport into the firn mainly comes from heat advection/diffusion and water percolation [*Suter*, 2002; *Vincent et al*., 2007b]. The amount of melt energy depends on the surface energy balance which, given the high relevance of shortwave radiation, is highly dependent on elevation, slope, aspect, and albedo. The resulting near-surface firn temperature is therefore highly spatially variable [*Suter et al*., 2001]. Consequently, a very high spatial variability in firn or ice temperatures is observed at these very high elevation areas [*Hoelzle et al*., 2011]. In addition to these factors, the deep englacial temperatures also depend on ice and firn advection, firn conductivity and basal heat flux [*Lüthi and Funk*, 2001].

[4] A major challenge of reconstructing past temperatures from ice temperature profiles is the separation of thermal changes due to air temperature from those due to other sources. *Gilbert et al*. [2010] successfully reconstructed air temperature over the last century at Illimani (Bolivia, 6340 m a.s.l.) from one single englacial temperature profile using complementary data such as ice core density and stratigraphy to quantify the melting intensity and firn advection.

[5] In this study, we reconstruct an air temperature signal over the last century from seven englacial temperature profiles at very high altitudes between 4240 and 4300 m a.s.l.

Additional Supporting Information may be found in the online version of this article.

[1]UJF-Grenoble 1 / CNRS, LGGE UMR 5183, Grenoble cedex 09, France.

Corresponding author: A. Gilbert, UJF-Grenoble 1 / CNRS, LGGE UMR 5183, BP 96, 38041 Grenoble cedex 09, France. (gilbert@ujf-grenoble.fr)

0094-8276/13/10.1002/grl.50401

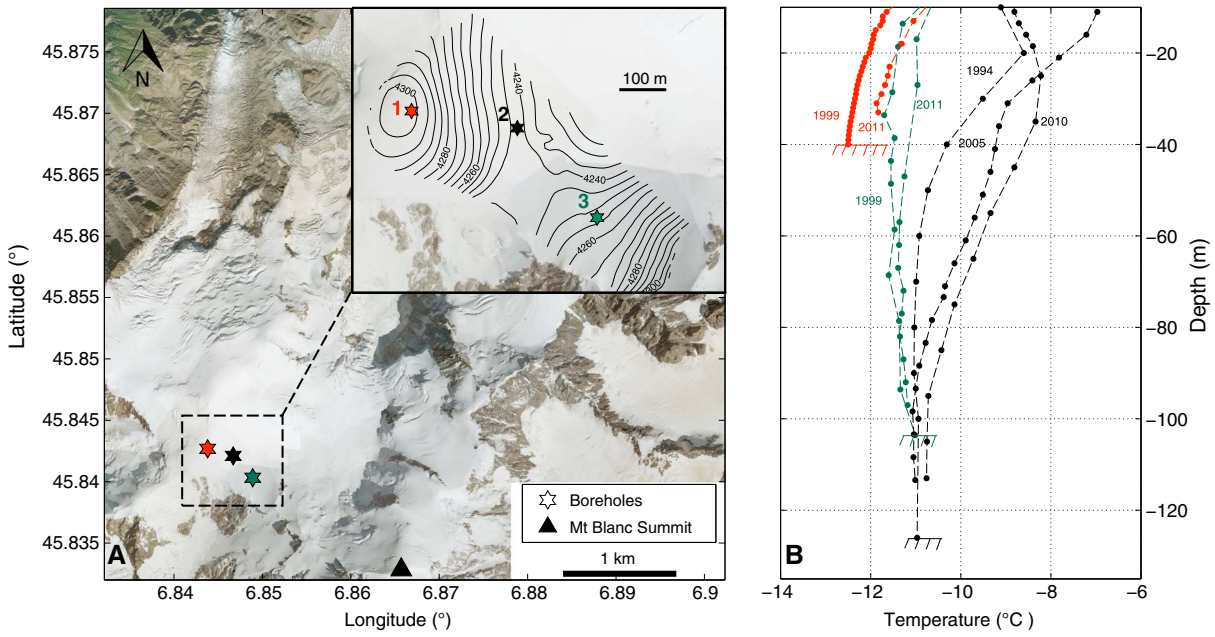

Figure 1. (a) Aerial view of the studied area with a zoom on the drilling site. Numbers indicate the three borehole drilling sites. (b) Ice temperature measurements in boreholes shown in Figure 1A with corresponding colors.

in the Mont Blanc area. This reconstruction is compared to air temperatures observed at lower altitudes. This method was also used to identify criteria that can be used to select the best drilling sites to infer past air temperatures from englacial temperatures.

2. Measurements

[6] Englacial temperature measurements were performed from the surface to bedrock in seven boreholes drilled between 1994 and 2011 at three different sites in the Mont Blanc area located between 4240 and 4300 m a.s.l. (Figure 1). At 4240 m, the mean annual air temperature is –10 °C and summer temperatures rarely exceed 0°C. Ice thicknesses were 40, 126, and 103 m at sites 1, 2, and 3, respectively. The accuracy of all temperature sensors was better than ±0.1°C except for the 1999 profile at site 3 for which the accuracy was ±0.3°C due to a calibration problem. The boreholes were drilled using electro-mechanical equipment up to 1999 (included) and subsequently by hot water drilling. Measurements were repeated in each borehole several times after drilling until a thermal equilibrium (+/–0.05°C) was reached. The ice temperature measurements are shown in Figure 1 and the aspect, slope and elevation of the borehole locations are reported in Table 1. The ice temperature changes exhibit a high spatial variability. Indeed, although sites 2 and 3 are very close (250 m) and at the same elevation (about 4250 m a.s.l.), temperature changes over the last 10 years are very different, for example 0.4°C and 1.2°C at 40 m depth for sites 3 and 2, respectively.

[7] Firn and ice densities were measured on ice cores at all three sites from the surface to bedrock. Horizontal and vertical velocities (v_h and v_0, respectively) were measured by differential GPS surveys over the period 1993–2010 at all three sites (Table 1). The high spatial variability of snow accumulation is responsible for the very high spatial variability of the subsidence velocity [*Vincent et al.*, 2007a].

3. Methodology

3.1. Forward Model

[8] To reconstruct the past atmospheric temperature changes, we used a forward model to simulate englacial temperatures from air temperature variations [*Gilbert et al.*, 2010]. We assume that horizontal heat advection can be neglected due to very low horizontal velocity (Table 1). This assumption is supported by three-dimensional numerical experiments (see supporting information). Therefore, we solve the heat diffusion/advection problem at each site in firn and ice in one dimension by solving the heat transfer equation [*Malvern*, 1969; *Hutter*, 1983]

$$\rho c_p\left(\frac{\partial T}{\partial t}+v_z\frac{\partial T}{\partial z}\right)=\frac{\partial}{\partial z}\left(k\frac{\partial T}{\partial z}\right)+Q_{\text{lat}} \qquad (1)$$

where z is the depth (m), t the time (s), T the temperature (K), c_p the heat capacity of ice (= 2030 J kg^{-1} K^{-1}), ρ the firn density (kg m^{-3}), v_z the vertical advection velocity (m s^{-1}), k the thermal conductivity of firn (W m^{-1} K^{-1}) and Q_{lat} the latent heat released by refreezing meltwater (W m^{-3}).

Table 1. Borehole Site Characteristics

Site No.	Elevation (m a.s.l.)	Depth (m)	Firn thickness (m)	Aspect	Slope(°)	Measurement Dates	Horizontal Velocities (m yr^{-1})	Subsidence Velocities (m w.e. yr^{-1})
1	4300	40	20	E	8	1999 / 2011	1.2	0.7
2	4245	126	80	E	10	1994 / 2005 / 2010	7.9	3.2
3	4255	103	60	NW	10	1999 / 2011	3.5	1.3

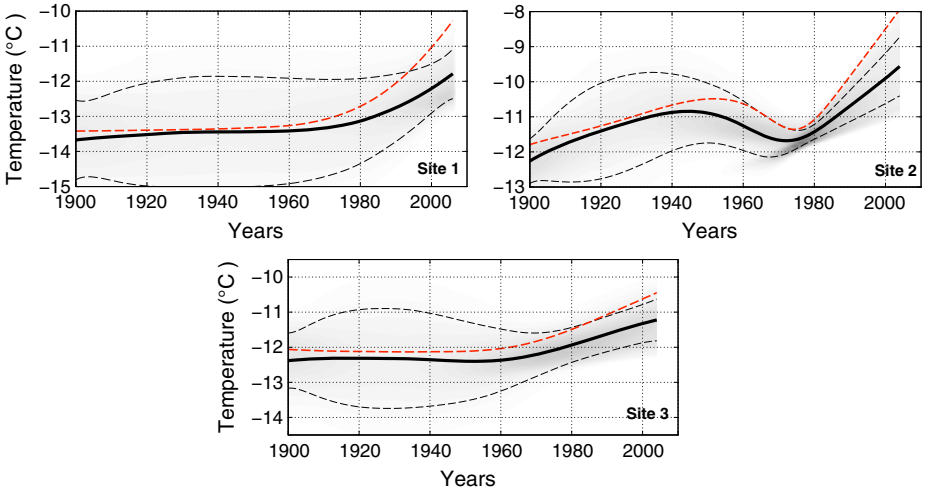

Figure 2. Posterior PDF of air temperature sampled by RJ-MCMC algorithm for each borehole. The thick line shows the mean posterior PDF and the dashed line is the standard deviation. The red dashed line shows mean posterior PDF for inversion of firn surface temperature.

Equation (1) is solved using the spectral element method [*Patera*, 1984] with a time step of one year. We use measured densities at sites 1, 2, and 3. Conductivity is inferred from density using the relationship given by *Calonne et al.* [2011] based on experimental measurements and numerical simulation using microtomographic images. The basal heat flux f_b is given at 800 m depth in the bedrock. At this depth, the basal heat flux is assumed to be constant during time of the simulation (see supporting information). The thermal properties of the bedrock (gneiss and granite) are not well known. We use a thermal conductivity of 3.2 $W\,m^{-1}\,K^{-1}$, a heat capacity of 7.5 $10^2\,J\,kg^{-1}\,K^{-1}$ and a density of 2.8 $10^3\,kg\,m^{-3}$ as proposed by *Lüthi and Funk* [2001]. The annual surface temperature T_s is assumed to vary in the same way as the mean annual air temperature [*Gilbert et al.*, 2010]. The latent flux from refreezing of meltwater is released at the surface and calculated from an annual temperature anomaly:

$$Q_{\mathrm{lat}} = \frac{a(T_s - T_{\mathrm{ref}})L\rho_w}{h} \tag{2}$$

where T_{ref} (K) is equal to the steady state temperature T_0 (K) (see next section), L (3.34 $10^5\,J\,kg^{-1}$) is the latent heat of fusion, a (m w.e. $K^{-1}\,s^{-1}$) a melting factor (different for each site), ρ_w (= 1.0 $10^3\,kg\,m^{-3}$) the water density and h (m) a scale factor representing the thickness of the layer influenced by latent heat over one year ($h = 10$ m here). The vertical advection profile is calculated from the surface advection velocity v_0 (m w.e. yr^{-1}) and assumed to vary linearly with depth [*Vincent et al.*, 2007b]

$$v_z(z) = \frac{v_0\rho_w}{\rho(z)}\left(1 - \frac{z}{D}\right) \tag{3}$$

where z is depth (m), D the bedrock depth (m), ρ_w the water density ($kg\,m^{-3}$) and $\rho(z)$ the firn density.

3.2. Inverse Problem

[9] The inverse problem is solved using Bayesian inference [*Hopcroft et al.*, 2007] via the method used by *Gilbert et al.* [2010]. We use a Reversible Jump Markov Chain Monte Carlo (RJ-MCMC) algorithm to explore the parameter space and randomly draw the posterior probability density function (PDF) of each parameter. At every site, five different parameters are explored: the surface temperature evolution vector **Ts**, the melting factor a (equation (2)), the basal flux f_b, the surface advection velocity v_0 and the steady state surface temperature T_0 used to compute the initial profile. As proposed in other studies [e.g., *Lüthi and Funk*, 2001], a long past temperature history is used to calculate the initial temperature profile in 1900. For this purpose, numerical modeling experiments start in the year 800 for which we assume a steady state profile. Numerical experiments have shown that this past temperature history has a very small influence on the temperature inversion (see supporting information). This initial profile is calculated for every iteration of the RJ-MCMC algorithm using T_0 and v_0. The surface temperature evolution is represented by a series of linear segments with the nodes of these segments being the model parameters **Ts**, i.e., $\mathbf{Ts} = (T_k\ ,\ t_k;\ k = 1,5)$, where T_k is

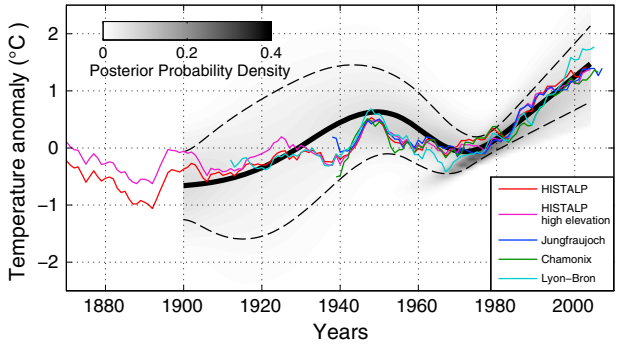

Figure 3. Air temperature variations in the Mont Blanc area over the last century from simultaneous inversion using all boreholes (black bold line). The colored curves are the time series of the 10 year moving averages of air temperature from Chamonix (1050 m a.s.l.), Lyon-Bron (200 m a.s.l.) and Jungfraujoch (3570 m a.s.l.) meteorological stations and from HISTALP and HISTALP high elevation (1500 to 3500 m a.s.l.) reconstitutions in the northwestern Alps [*Auer et al.*, 2007].

Table 2. Posterior PDF Means and Standard Deviations of Mean Latent Heat (Q_{lat}), Subsidence Velocities (v_0), Basal Heat Flux (f_b) and Steady State Temperature (T_0) as Sampled by the RJ-MCMC Algorithm in the Simultaneous Inversion

	Steady State Temperature	Mean Latent Flux	Subsidence Velocities	Basal Heat Flux
Site No.	T_0 (°C)	Q_{lat} (mW m^{-3})	v_0 (m w.e. yr^{-1})	f_b (10^{-3} W m^{-2})
1	-14.4 ± 0.5	30 ± 16	0.6 ± 0.4	25 ± 16
2	-12.4 ± 0.5	32 ± 16	3.7 ± 0.2	26 ± 16
3	-12.7 ± 0.5	7 ± 10	1.1 ± 0.4	36 ± 12

temperature and t_k is time. Posterior PDF is calculated for each parameter set sampled by the RJ-MCMC algorithm following the Bayesian approach:

$$P_{post} \propto P_{prior} \times P(\mathbf{d} \mid \mathbf{m}) \quad (4)$$

where P_{post} is the posterior PDF, P_{prior} is the prior PDF and P($\mathbf{d} \mid \mathbf{m}$) is the probability of observing the data d for a given parameter set m. Details on the calculation of the posterior PDF are given in the supplementary material.

[10] In order to deal with the three sites simultaneously, the surface temperature is defined as a deviation from the steady state temperature T_0 (different at each site). The surface temperature evolution vector **Ts** is the same for all sites and the surface temperature at each site is given by:

$$\mathbf{T}_\mathbf{s}^i = \mathbf{T}_\mathbf{s} + T_0^i \quad (5)$$

where $\mathbf{Ts}^i$ is the surface temperature at site i and ${T_0}^i$ the steady state temperature at site i. Data likelihood is calculated as the product of the data likelihood at each site

$$P(\mathbf{d}_{i=1,3} \mid \mathbf{m}_{i=1,3}) = \prod_{i=1}^{3} P(\mathbf{d}_i \mid \mathbf{m}_i) \quad (6)$$

where $\mathbf{d}_i$ is the data at site i and $\mathbf{m}_i$ the parameters set for site i.

4. Results

4.1. Individual Inversion at Each Site

[11] Atmospheric temperature reconstruction at each site is shown in Figure 2. Ten million iterations were needed to reach a steady posterior PDF. The mean value of the posterior PDF (black bold line) is interpreted as the expected value given by the inversion. The standard deviation (or 68% credible interval) gives the uncertainty (thin dashed line). The three inversions exhibit an air temperature rise starting between 1960 and 1980. The mean warming amplitude between 1960 and 2004 is 1.4°C with a warming of 1.6°C, 1.4°C, and 1.1 °C for sites 1, 2, and 3, respectively. The sites are too close to experience such different air temperature warming and the differences observed here are clearly due to uncertainties inherent to the method. The uncertainty of these reconstructions remains high due to the uncertainties associated with the melting intensity and advection velocity at each site. Our analysis shows that repeated measurements at the same site and at different times significantly improve the accuracy of reconstruction. For instance, the three measurements performed in 1994, 2005, and 2010 at site 2 provide the most accurate reconstruction of air temperatures (Figure 2). Moreover, the high advection velocity and melting intensity found at this site increase the impact of the atmospheric temperature change on englacial temperatures and provides a better reconstruction. Note that the englacial temperature measurements carried out in this borehole make it possible to detect the warm period of the 1940s. The reconstruction from borehole 1 temperatures does not provide any information before 1970 due to the low thickness of the glacier at this site. For site 3, high-frequency climate variations are filtered out by diffusion as a result of the low advective heat transfer. No trace of the forties warm period can therefore be detected from temperature profiles measured at site 3.

[12] A second set of inversion experiments were performed assuming no melting/refreezing processes at the surface (i.e., $a = 0$ in equation (2)), making it possible to

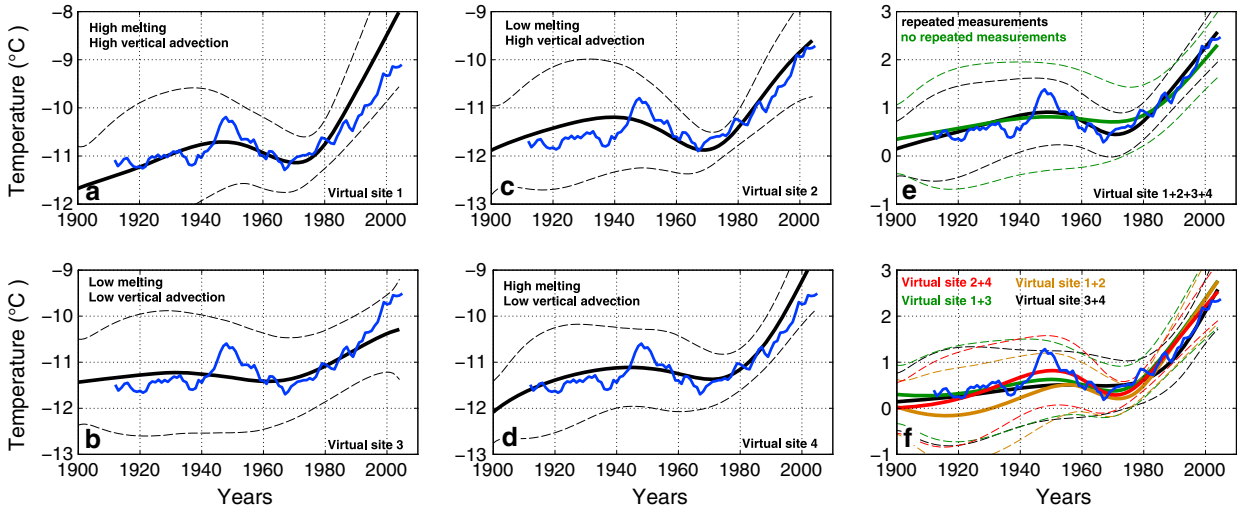

Figure 4. Inversions of synthetic englacial temperature profiles created from the forward model forced by daily air temperature measured at Lyon-Bron and using different melting intensities and advection velocities. Bold lines are the mean posterior PDF and dashed lines are the standard deviation of each inversion. The blue line is the 10 year moving average of Lyon-Bron temperature.

Table 3. Comparison of Atmospheric Temperature Trends From the Different Data Sets

	Elevation Range	Localization	Type of Data	Linear Trend 1900–2004 (K decade^{-1})	Linear Trend 1960–2004 (K decade^{-1})	Linear Trend 1980–2004 (K decade^{-1})
HISTALP	0–3500 m a.s.l.	NW Alps	Homogenized records	0.14	0.36	0.58
HISTALP high elevation	1500–3500 m a.s.l.	Alps	Homogenized records	0.12	0.36	0.50
Jungfraujoch	3570 m a.s.l.	46°32′ 7°58′	Meteorological station	-	0.35	0.52
Lyon-Bron	200 m a.s.l.	45°72′ 4°94′	Meteorological station	-	0.46	0.72
Chamonix	1042 m a.s.l.	45°93′ 6°88′	Meteorological station	-	0.31	0.51
This study	4250 m a.s.l.	45°84′ 6°84′	-	**0.14 ± 0.06**	**0.33 ± 0.02**	**0.55 ± 0.15**

reconstruct surface firn temperature variations (Figure 2, red dashed curve). Comparison with the atmospheric temperature reconstruction (Figure 2, black bold curve) shows the occurrence of surface melting at each site when atmospheric and firn temperature variations deviate. At site 2, the reconstructed surface firn temperature rises by 3.3°C over the last 30 years while reconstructed atmospheric temperature rises by 1.8°C. This confirms the strong impact of increasing melting on englacial temperature in cold glaciers as already demonstrated by other studies [*Vincent et al.*, 2007b; *Suter et al.*, 2001; *Lüthi and Funk*, 2001; *Gilbert et al.*, 2010].

4.2. Simultaneous Inversion

[13] Simultaneous inversion provides a way to reduce uncertainties related to the melting intensity inference and greatly increases the reliability of the reconstruction (see the numerical experiments performed with the synthetic englacial data set, in section 5). Simultaneous inversion results are shown in Figure 3 and Table 2 (mean posterior PDF and standard deviation of all parameters for each site) assuming the same temperature changes at the three sites. Posterior PDFs of a, v_0 , f_b, and T_0 are shown in the supporting information. The surface temperature is given here as a deviation from steady state temperature T_0 at each site (equation (5)). This method improves the accuracy of the reconstruction and reduces the uncertainty of parameter estimation given that the same temperature evolution explains englacial temperature changes for all the three sites. Fifty million iterations were needed to reach a steady posterior PDF.

[14] Results exhibit a 1.2°C warming between 1900 and 1950, a cooling period of 0.7°C between 1950 and 1975, and a recent 1.6°C warming between 1975 and 2004. For each site, the inferred surface vertical velocity (v_0, Table 2) has been compared with GPS measurements [*Vincent et al.*, 2007a] (Table 1). This comparison shows good agreement for the three sites. Advection velocity profile (equation (3)) was also validated using ice core dating from radioactive horizons (see supporting information). Variation of melting intensity is linked to the slope and aspect of the site that influence the incoming potential solar radiation [*Suter*, 2002]. Thus, sites 1 and 2 are more subject to surface melting than site 3. This is consistent with our inversion results (Table 2) that show less energy released by refreezing of meltwater at site 3.

[15] The reconstructed basal flux values seem to show a stronger basal flux at site 3. This could be due to topographical effects related to the influence of the south face of Mont Blanc.

5. Sensitivity and Reliability of Temperature Reconstructions

[16] The accuracy of temperature reconstructions is very sensitive to the choice of drilling sites. As shown in section 4.1, the main parameters that influence the reconstruction are the melting intensity driven by the local incoming potential solar radiation [*Suter*, 2002] and the firn vertical advection velocity driven by the seasonal distribution of accumulated snow [*Vincent et al.*, 2007a].

[17] To test the reliability of our reconstruction, we investigated the influences of melting intensity and vertical advection velocity using a synthetic englacial data set. This data set was obtained from the forward model forced by the daily air temperature measured at Lyon-Bron meteorological station and different values of vertical advection velocity and melting intensity. Melting is calculated using the classical degree-day method at a daily time scale [e.g., *Hock*, 2003]. Four virtual sites were created using low and high vertical advection (set to 0.5 and 4.0 m w.e. yr^{-1}, respectively) and low and high melting intensity (with degree-day factor set to 0 and 2.0 mm K^{-1} d^{-1}, respectively). For each virtual site, we modeled three virtual 126 m deep englacial temperature profiles (in 1994, 2005, and 2010). Then air temperature was reconstructed from these profiles using the inverse method and compared with the temperatures from Lyon-Bron (Figures 4a to 4d). The deviation between reconstructed profiles and Lyon-Bron daily temperatures allows us to assess the reliability of the reconstruction. Results show high differences between Lyon-Bron temperature and reconstructions from individual inversion at each virtual site. These differences are due to the high uncertainty on the melting intensity which leads to a high uncertainty on the temperature reconstruction. In contrast, the use of simultaneous inversions at the four virtual sites reconstructs past temperature variations accurately (Figure 4e). In addition, our numerical experiments show that repeated measurements at the same site reduce significantly the uncertainty of the reconstruction (Figure 4e).

[18] Some further experiments were performed to test the best combination of measurements for temperature reconstruction (Figure 4f). These experiments show that the use of only two sites is sufficient to obtain reliable temperature reconstruction. They also reveal that the best reconstruction

is obtained from sites with contrasting melting intensity and accumulation (Figure 4f). The use of two sites overcomes the difficulty of inferring melting from englacial temperature measurements. Conversely, reconstructions based on only one site require independent calibration of melting factor from direct measurements or from an energy balance model using on-site automatic weather station data. In addition to a sensitivity analysis, these numerical modeling experiments show that the air temperature reconstruction shown in Figure 3 is relevant.

6. Discussion and Conclusions

[19] For the first time, atmospheric temperatures over 100 years were reconstructed at a very high elevation using multiple englacial temperature profiles. This reconstruction does not depend on any air temperature record from lower elevations. Our results exhibit a warming of 2.0 ± 0.6°C with a linear trend of 0.14 ± 0.06°C/decade at around 4300 m a.s.l. in the Mont Blanc area between 1900 and 2004. The 2°C warming corresponds to the reconstructed temperature difference between 1900 and 2004. This confirms that 20th century warming in the Alps was greater than the global and hemispheric average [*Beniston et al*., 1997]. These results have been compared to local meteorological data and temperature reconstructions from HISTALP [*Auer et al*., 2007] (Figure 3). Local meteorological data have been recorded in the valley at Chamonix (1050 m a.s.l.) since 1934, in the plain at Lyon-Bron meteorological station (200 m a.s.l.) since 1907 (located 200 km west of the glacier) and at Jungfraujoch meteorological station (3570 m a.s.l., Switzerland) since 1933. *Auer et al*. [2007] used measurement instrument series (mostly located below 1500 m a.s.l.) of monthly mean temperature to estimate the homogenized long-term temperature evolution in the Alps. The means for the northwestern Alps and the selected high elevation data set temperatures (1500 to 3500 m a.s.l.) are reported in Figure 3 together with the inversion results. Temporal temperature trends relative to these series are shown in Table 3. We can conclude that our reconstruction is in good agreement with the temperature trends of all these data over all the different periods 1900–2004, 1960–2004, and 1980–2004. Only Lyon-Bron temperature trend seems to be stronger over the periods 1960–2004 and 1980–2004. A possible effect of urbanization could affect this series [*Pepin and Lundquist*, 2008]. The good agreement with temperatures trends from HISTALP confirms that temperature change at very high elevations in the Mont Blanc area is representative of a regional climate change and it is not biased by local effects. We conclude that atmospheric temperature trends detected on Mont Blanc above 4000 m a.s.l. agree fairly well with the trends recorded at lower elevations or reconstructed at regional scale, even though they have been obtained fully independently from these records. This suggests that, in the Alps, warming is not increasing at very high elevations above the 0°C isotherm.

[20] These results seem to conflict with modeling studies using future scenarios that have shown an elevation-dependent climate response [e.g., *Giorgi et al*., 1997, *Im et al*., 2010]. However, it is difficult to compare our results with other results from large-scale atmospheric modeling and simulations for the future. Studies based on ground observations during the 20th century show no overall agreement concerning the elevation dependency of atmospheric temperature trends [*Ceppi et al*., 2010; *Rangwala and Miller*, 2012; *Beniston and Rebetez*, 1996; *Jungo and Beniston*, 2001]. Our study suggests that there is a similar air temperature trend at low and very high altitudes over the last 100 years.

[21] Englacial temperature measurements provide a way to infer air temperature changes at very high elevations. We show that temperature reconstructions from englacial temperatures need a minimum of two neighboring measurement sites with contrasting surface melting and snow accumulation. This facilitates differentiation between the fraction of the englacial warming coming from increasing air temperature and the fraction coming from increasing surface melting. This method could be applied to other high elevation glaciated areas where meteorological data are nonexistent.

[22] **Acknowledgments.** This study was funded by the AQWA European program (212250). We thank P. Possenti and P. Ginot for conducting the drilling operation. We thank HISTALP project members for providing the homogenized instrument data in the Alps. We thank MétéoSwiss and Météo-France for providing air temperature data.

[23] The Editor thanks Martin Luthi, Shin Sugiyama and 1 anonymous reviewer for their assistance in evaluating this paper.

References

Auer, I., et al. (2007), HISTALP – Historical instrumental climatological surface time series of the greater Alpine region, *Int. J. Climatol.*, *27*, 17–46, doi:10.1002/joc.1377.

Beniston, M., H. F. Diaz, and R. S. Bradley (1997), Climatic change at high elevation sites: an overview, *Clim. Chang.*, *36*(3-4), 233–251.

Beniston, M., and M. Rebetez (1996), Regional Behavior of Minimum Temperatures in Switzerland for the Period 1979-1993, *Theor. Appl. Climatol.*, *53*, 231–243.

Calonne, N., F. Flin, S. Morin, B. Lesaffre, S. Rolland du Roscoat, and C. Geindreau (2011), Numerical and experimental investigations of the effective thermal conductivity of snow, *Geophys. Res. Lett.*, *38* (L23501), doi:10.1029/2011GL049234.

Ceppi, P., S. C. Scherrer, A. M. Fischer and C. Appenzeller (2010), Revisiting Swiss temperature trends, *Int. J. Climatol.*, *32*, 203–213, doi:10.1002/joc.2260.

Gilbert, A., P. Wagnon, C. Vincent, P. Ginot, and M. Funk (2010), Atmospheric warming at a high elevation tropical site revealed by englacial temperatures at Illimani, Bolivia (6340 m a.s.l., 16° S, 67° W), *J. Geophys. Res.*, *115* (D10109), doi:10.1029/2009JD012961.

Giorgi, F., J. W. Hurrell, M. R. Marinucci, and M. Beniston (1997), Elevation Dependency of the Surface Climate Change Signal: A Model Study, *J. Climate*, *10*, 288–296. doi:10.1175/1520-0442(1997)010 < 0288:EDOTSC 2.0.CO;2.

Hock, R. (2003), Temperature index melt modelling in mountain areas, *J. Hydrol.*, *282*(1–4), 104–115, doi:10.1016/S0022-1694(03)00257-9.

Hoelzle, M., G. Darms, M. P. Lüthi, and S. Suter (2011), Evidence of accelerated englacial warming in the Monte Rosa area, Switzerland/Italy, *The cryoshere*, *5*, 231–243, doi:10.5194/tc-5-231-2011.

Hopcroft, P. O., K. Gallagher, and C. C. Pain (2007), Inference of past climate from borehole temperature data using bayesian reversible jump markov chain monte carlo, *Geophys. J. Int.*, *171*, 1430–1439, doi:10.1111/j.1365-246X.2007.03596.X.

Hutter, K. (1983), *Theoretical Glaciology: Material Science of Ice and the Mechanics of Glaciers and Ice Sheets*, D. Reidel, Dordrecht, Netherlands.

Im, E.-S., E. Coppola, F. Giorgi, and X. Bi (2010), Local effects of climate change over the Alpine region: A study with a high resolution regional climate model with a surrogate climate change scenario, *Geophys. Res. Lett.*, *37*, L05704, doi:10.1029/2009GL041801.

Intergovernmental Panel on Climate Change (IPCC) (2007), Climate Change 2007: The Physical Science Basis. *Contribution of Working Group I to the Fourth Assessment Report of the Intergovernmental Panel on Climate Change*, edited by S. Solomon et al., Cambridge Univ. Press, Cambridge, UK.

Jungo, P., and M. Beniston (2001), Changes in the anomalies of extreme temperature anomalies in the 20th century at Swiss climatological stations located at different latitudes and altitudes, *Theor. Appl. Climatol.*, *69*, 1–12.

Lüthi, M., and M. Funk (2001), Modeling heat flow in a cold, high-altitude glacier: Interpretation of measurements from Colle Gnifetti, Swiss Alps, *J. Glaciol.*, *47*(157), 314–323. doi:10.3189/172756501781832223.

Malvern, L. E. (1969), *Introduction to the Mechanics of Continuous Medium*, Prentice Hall, Englewood Cliffs, N. J.

Messerli, B. and J. D. Ives (eds.) (1997), Mountains of the world: a global priority. The Parthenon Publishing Group.

Patera, A. T. (1984), A spectral element method for fluid dynamic laminar flow in a channel expansion, *J. Comput. Phys.*, *54*, 468–488.

Pepin, N. C. and J. D. Lundquist (2008), Temperature trends at high elevations: Patterns across the globe, *Geophys. Res. Lett.*, *35*, doi:10.1029/2008GL034026.

Rangwala, I. and J. R. Miller (2012), Climate change in mountains: a review of elevation-dependent warming and its possible causes, *Clim. Chang.*, *114*, 527–547, doi:10.1007/s10584-012-0419-3.

Suter, S., M. Laternser, W. Haeberli, M. Hoelzle, and R. Frauenfelder (2001), Cold firn and ice of high-altitude glaciers in the Alps: Measurements and distribution modeling, *J. Glaciol.*, *47*(156), 85–96.

Suter, S. (2002), Cold firn and ice in the Monte Rosa and Mont Blanc areas: spatial occurrence, surface energy balance and climatic evidence, PhD thesis, ETH Zürich.

Vincent, C., E. Le Meur, D. Six, M. Funk, M. Hoelzle, and S. Preunkert (2007a), Very high elevation Mont Blanc glaciated areas not affected by the 20th century climate change, *J. Geophys. Res.*, *112*, doi:10.1029/2006JD007407.

Vincent, C., E. Le Meur, D. Six, P. Possenti, E. Lefebvre, and M. Funk (2007b), Climate warming revealed by englacial temperatures at Col du Dôme (4250 m, Mont-Blanc area), *Geophys. Res. Lett.*, *34*, doi:10.1029/2007GL029933.